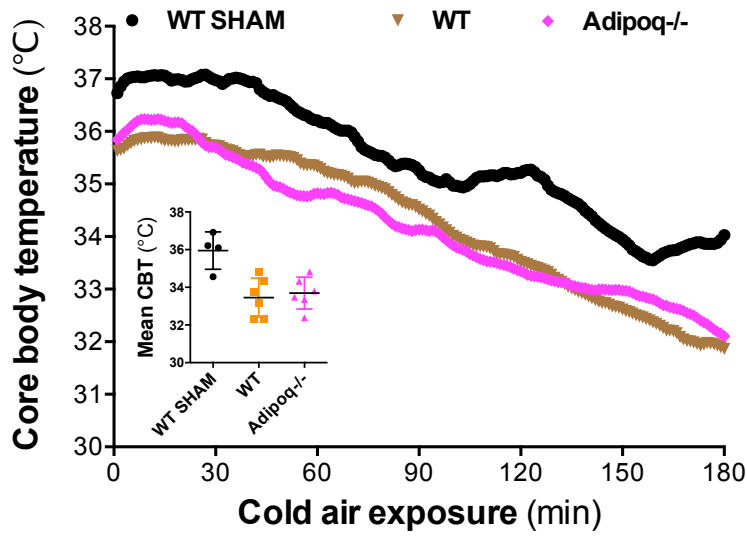
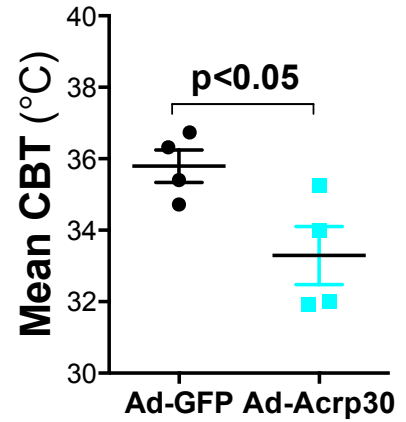


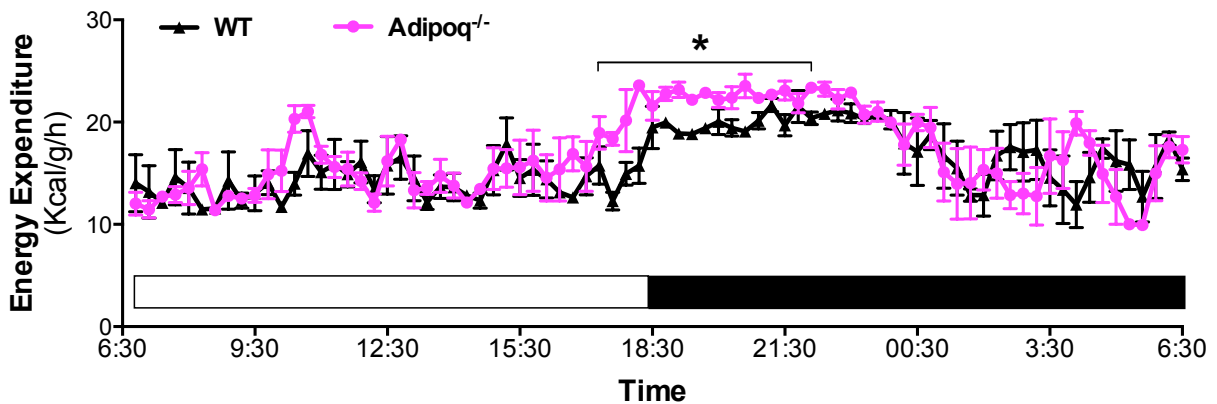
Suppl. Fig. 1A



Suppl. Fig. 1B

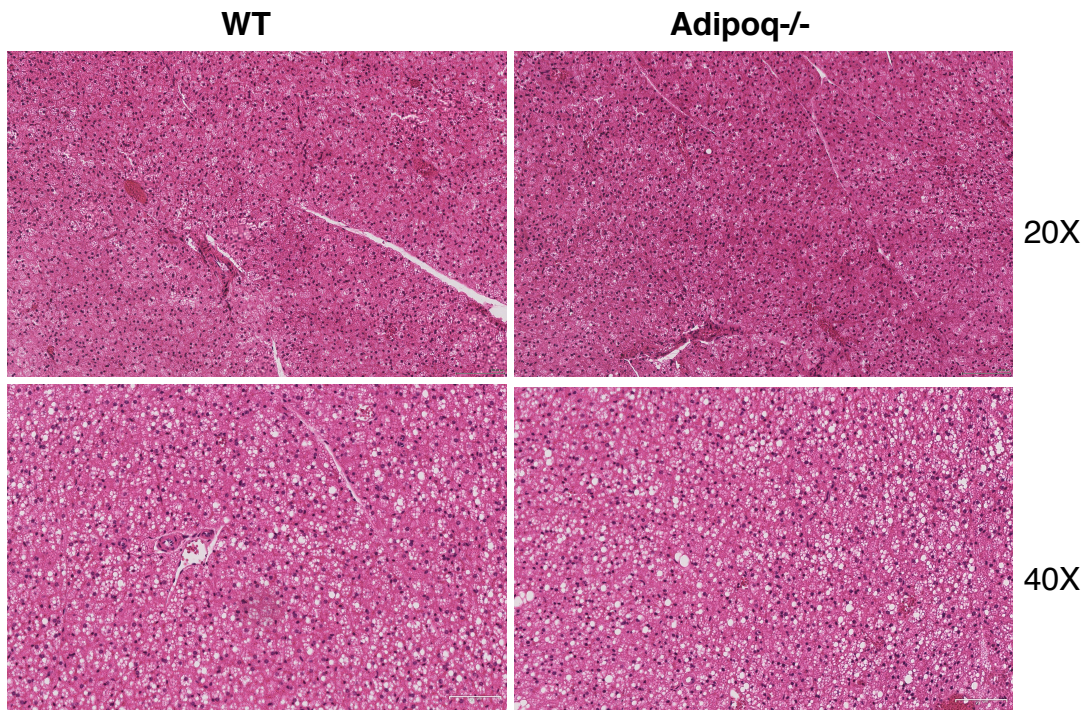


Suppl. Fig. 1C



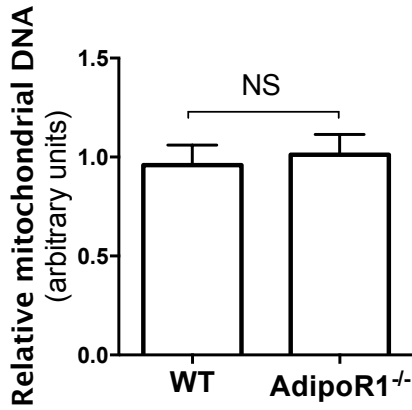
Supplemental figure 1. Adiponectin suppresses thermogenesis and energy expenditure. A, iBAT was surgically excised from WT and Adipoq^{-/-} mice, using sham-operated WT as control. After 1-week of recovery, CBT was measured during 3h acute cold exposure. B, adenovirus-mediated adiponectin reconstitution reduced CBT of Adipoq^{-/-} mice during acute cold exposure (4h). C, energy expenditure rates of Adipoq^{-/-} and WT mice were measured using indirect calorimetry and normalized to lean body mass, which was determined using EchoMRI.

Suppl. Fig. 2

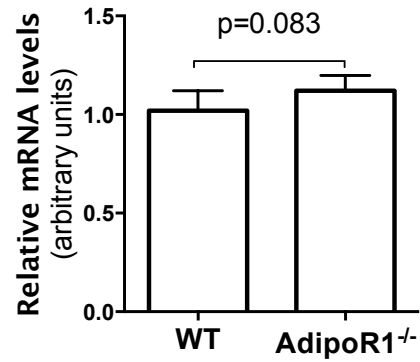


Supplemental figure 2. iBAT of Adipoq^{-/-} mice is histologically indistinguishable from WT control. The iBAT from male Adipoq^{-/-} and WT mice were collected after overnight fasting at room temperature. Sections were stained with H&E.

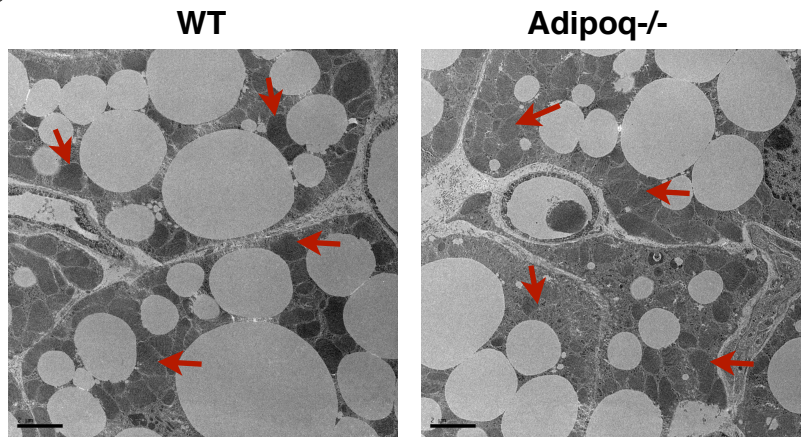
Suppl. Fig. S3A



Suppl. Fig. 3B

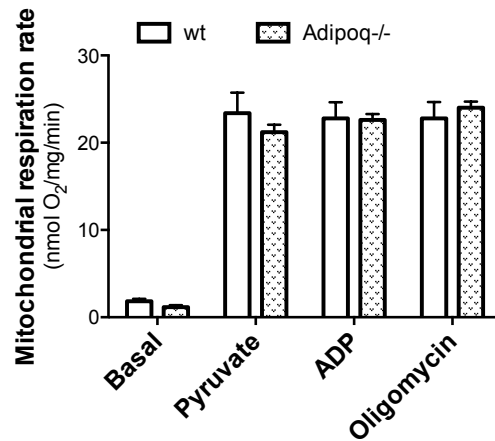
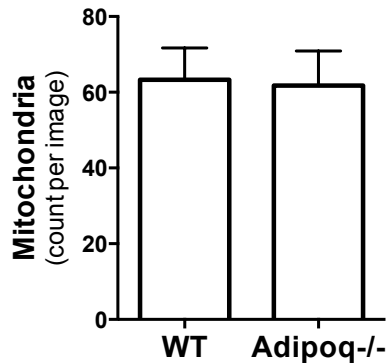


Suppl. Fig. 3C



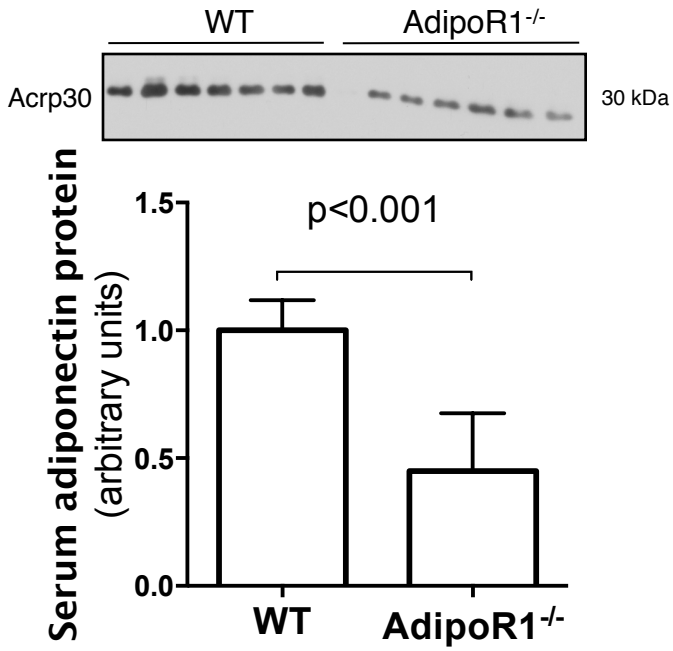
Suppl. Fig. 3E

Suppl. Fig. 3D

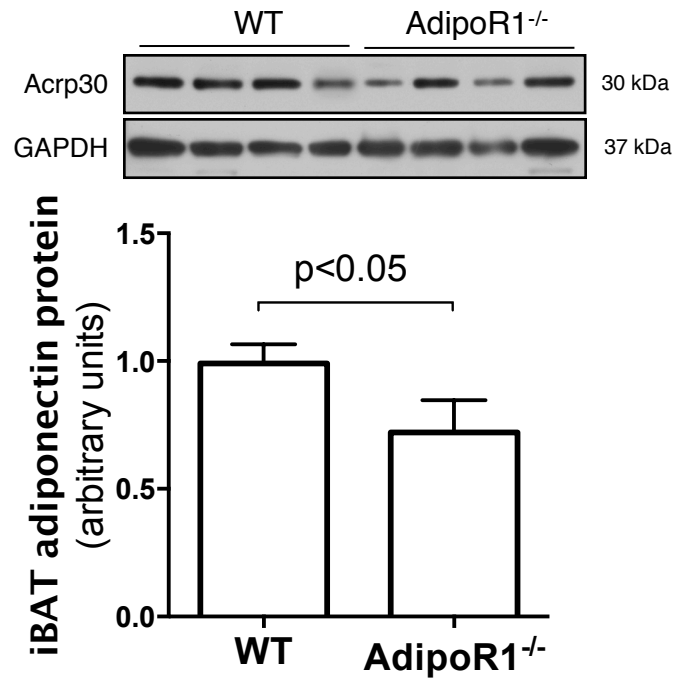


Supplemental figure 3. Effect of adiponectin on mitochondrial biogenesis and respiration. iBAT was collected from WT and Adipoq^{-/-} mice housed at room temperature. There were no difference in mitochondrial DNA (A), Cox5a mRNA levels (B), mitochondrial structure and density (C&D), and mitochondrial respiration rate using pyruvate as the substrate (E). The images of ultrastructure of iBAT were from electronic microscopy, and the scale bar is 2 μ m. Mitochondria were counted with randomly chosen images (n=10).

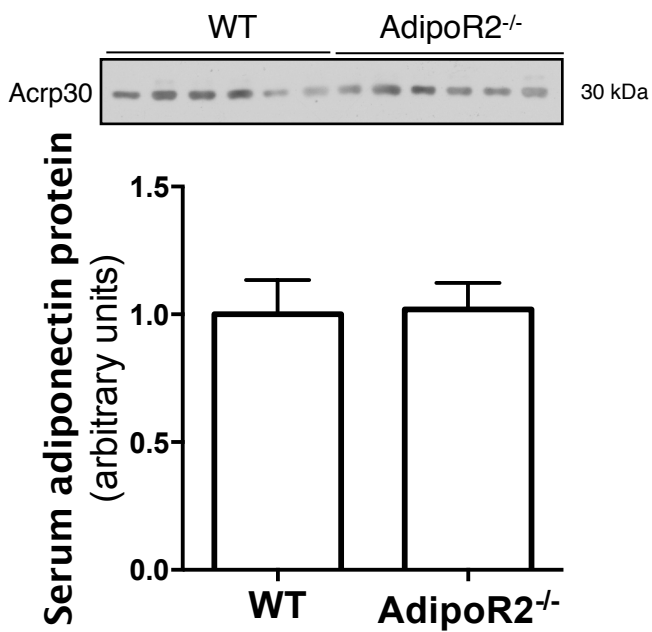
Suppl. Fig. 4A



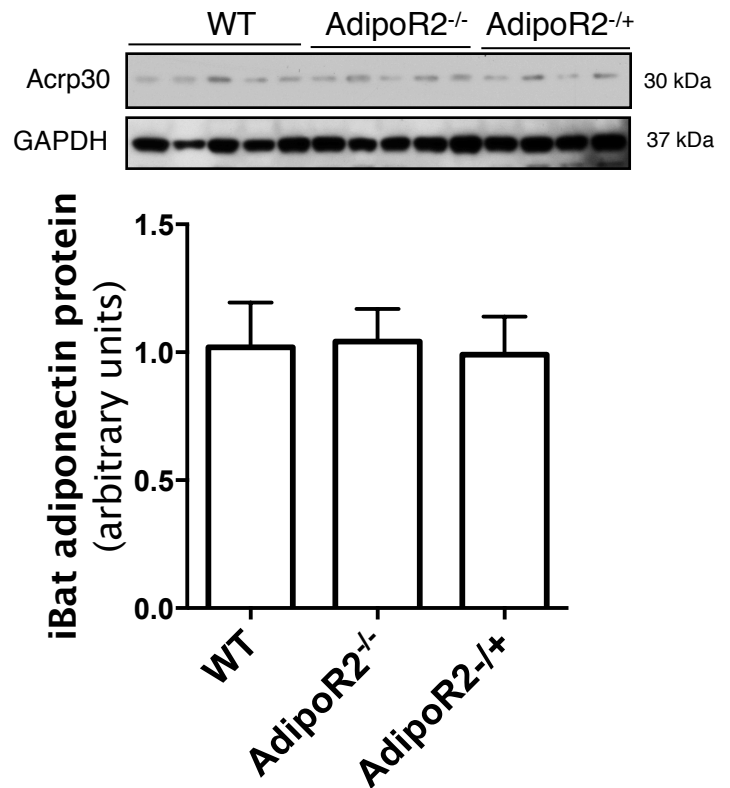
Suppl. Fig. 4B



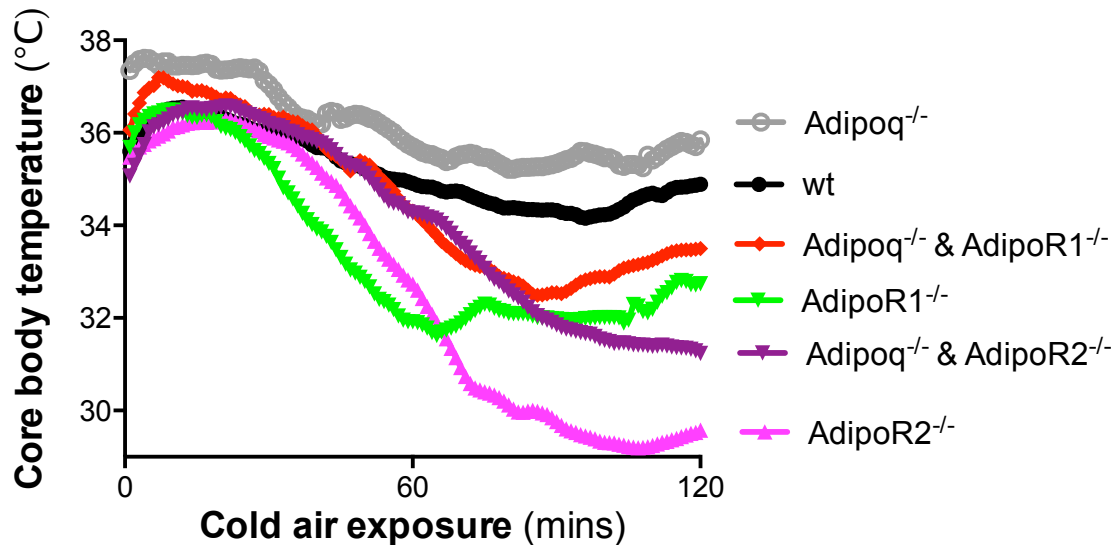
Suppl. Fig. 4C



Suppl. Fig. 4D

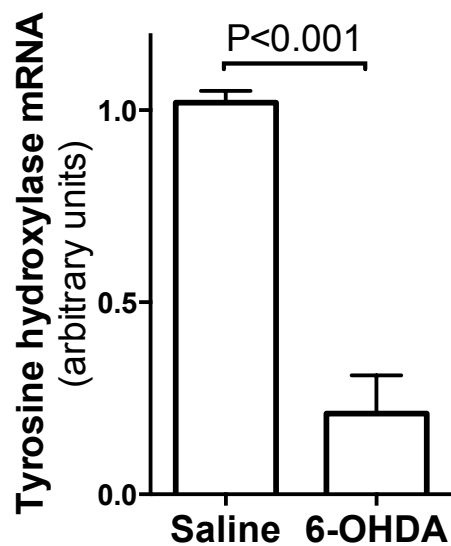


Suppl. Fig. 4E

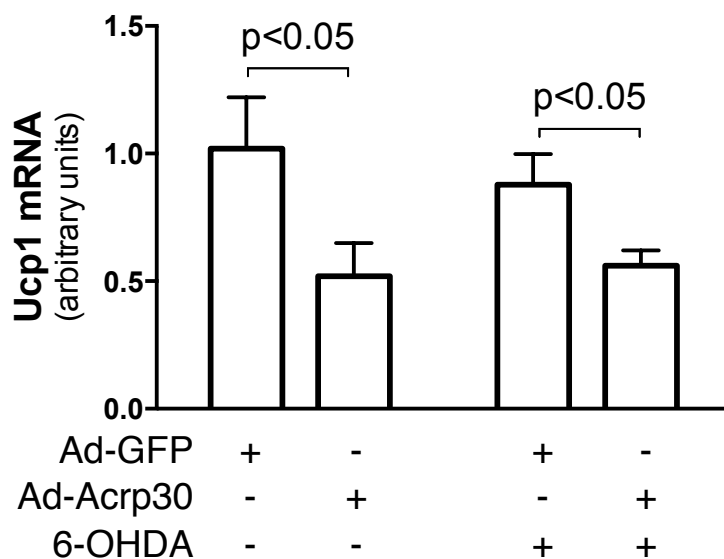


Supplemental figure 4. Adiponectin knockout in AdipoR1- or AdipoR2-deficient background alleviates hypothermia during cold exposure. A-D, AdipoR1^{-/-}, AdipoR2^{-/-}, AdipoR2^{-/+} and WT mice were housed at room temperature. Blood (A&C) and iBAT (B&D) were collected from in fasting state, and adiponectin was determined by immunoblotting. 4E, Adipoq^{-/-}&AdipoR1^{-/-} and Adipoq^{-/-}&AdipoR2^{-/-} double knockout mice (4-6 weeks old male, n=4-8 per group) were implanted with an emitter. After one week of recovery, CBT was monitored during a 2-hr exposure to 4 °C air.

Suppl. Fig. 5A

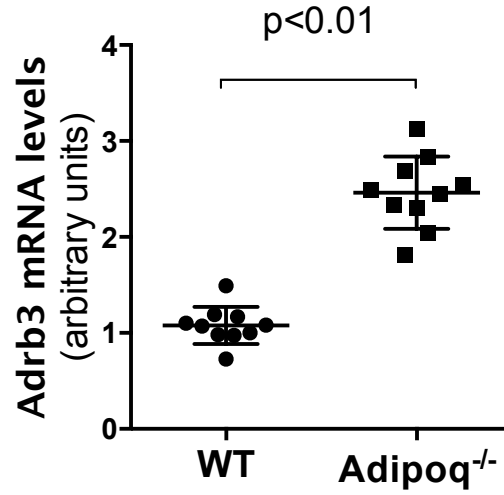


Suppl. Fig. 5B



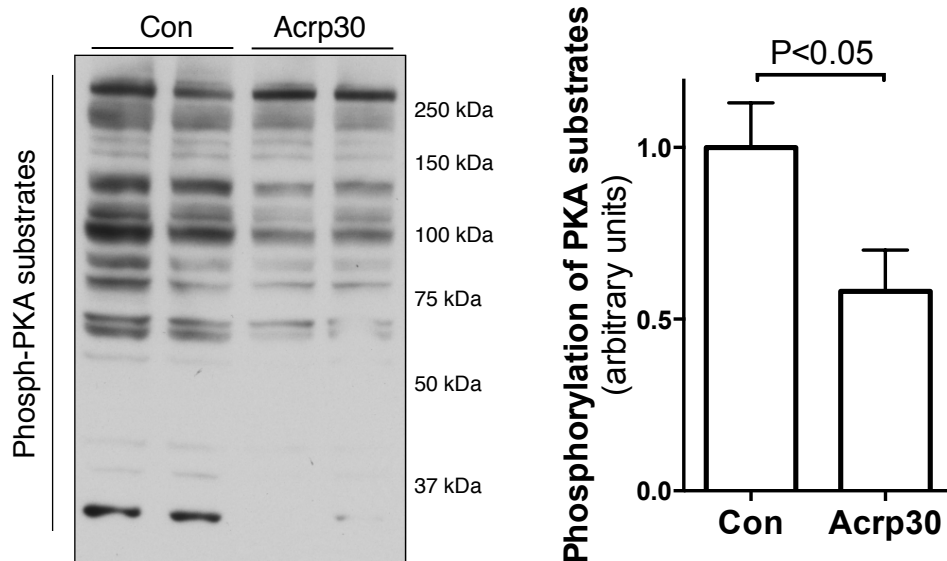
Supplemental figure 5. iBAT sympathetic denervation in *Adipoq*^{-/-} mice does not abolish the inhibitory effects of adiponectin on Ucp1 expression in iBAT. The neurotoxin 6-hydroxydopamine (6-OHDA) was injected into one side of iBAT of male *Adipoq*^{-/-} mice for sympathetic denervation. The contralateral iBAT were injected with saline as control. After 1 week of recovery, Ad-Acrp30 vectors were injected intravenously to reconstitute adiponectin, and iBAT were collected 3 days later to quantify tyrosine hydroxylase (A) and Ucp1 (B) mRNA by real-time PCR. n=5 per group.

Suppl. Fig. 6A

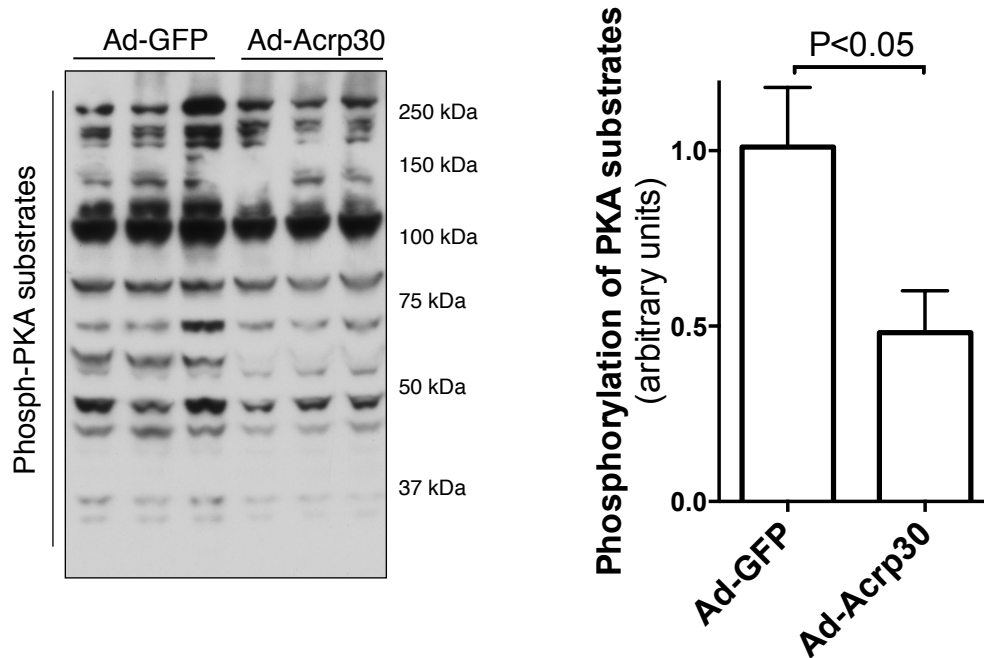


Supplemental figure 6A. Increased ADRB3 expression in inguinal fat of Adipoq^{-/-} mice. Inguinal fat pads were collected from Adipoq^{-/-} and WT control mice at RT. ADRB3 mRNA levels were quantified by real-time PCR.

Suppl. Fig. 6B



Suppl. Fig. 6C



Supplemental figure 6B&C. Adiponectin reduces PKA substrates phosphorylation in brown adipocytes and iBAT. B, brown adipocytes differentiated from stromal vascular fraction of iBAT of Adipoq^{-/-} mice were treated overnight with Acrp30 using a co-culture system. Protein samples were collected after 30 min treatment of ISO (10 μ M). C, Adipoq^{-/-} mice were transduced with Acrp30-expressing adenovirus to reconstitute adiponectin, using GFP adenovirus as control. iBATs were collected 3 days later. Phosphorylation of PKA substrates were detected by Western blotting using a specific antibody (#9621, Cell Signaling). The density of the bands of phosphorylated PKA substrates was quantified using Quantity One 1-D Analysis Software (BioRad Hercules, CA). For each sample lane, all bands between 250 – 25 kDa were selected and quantified, which represent the total level of phosphorylated PKA substrates of each sample. n=6 for each group.